

## Effect of methoxy group/s on D- $\pi$ -A porphyrin based DSSC: efficiency enhanced by co-sensitization

Devulapally Koteswar,<sup>1,2</sup> Seelam Prasanthkumar,<sup>1,2</sup> Surya Prakash Singh,<sup>1,2</sup> Towhid H. Chowdhury,<sup>3</sup> Idriss Bedja,<sup>4</sup> Ashraful Islam,<sup>3\*</sup> Lingamallu Giribabu,<sup>1,2\*</sup>

<sup>1</sup>*Polymers & Functional Materials Division, CSIR-Indian Institute of Chemical Technology, Tarnaka, Hyderabad-500007, India.*

<sup>2</sup>*Academy of Scientific and Innovative Research, CSIR-Indian Institute of Chemical Technology, India.*

<sup>3</sup>*Photovoltaic Materials Unit, National Institute for Materials Science, Sengen 1-2-1, Tsukuba, Ibaraki 305-0047, Japan. E-mail: [Islam.Ashraful@nims.go.jp](mailto:Islam.Ashraful@nims.go.jp)*

<sup>4</sup>*Cornea Research Chair, Optometry Department, College of Applied Medical Sciences, King Saud University, Riyadh 11433, Saudi Arabia*

*Corresponding authors: [giribabu@iict.res.in](mailto:giribabu@iict.res.in), [Islam.Ashraful@nims.go.jp](mailto:Islam.Ashraful@nims.go.jp) Phone: +91-40-27191724, Fax: +91-40-27160921;*

Table of Contents		Page No.
Figure S1	<i><sup>1</sup>H NMR spectrum (400 MHz, CDCl<sub>3</sub>) of D1</i>	S3
Figure S2	<i>ESI-MS of 1 (APPI-FTMS) D1</i>	S3
Figure S3	<i><sup>1</sup>H NMR spectrum (500 MHz, CDCl<sub>3</sub>) of D2</i>	S4
Figure S4	<i>ESI-MS of 1 (APPI-FTMS) D2</i>	S4
Figure S5	<i><sup>1</sup>H NMR spectrum (300 MHz, CDCl<sub>3</sub>) of 3</i>	S5
Figure S6	<i>MALDI-TOF of 3</i>	S5
Figure S7	<i><sup>1</sup>H NMR spectrum (300 MHz, CDCl<sub>3</sub>) of 4</i>	S6
Figure S8	<i>MALDI-TOF of 4</i>	S6
Figure S9	<i><sup>1</sup>H NMR spectrum (300 MHz, CDCl<sub>3</sub>+C<sub>5</sub>D<sub>5</sub>N) of LG24.</i>	S7
Figure S10	<i>MALDI-TOF of LG24.</i>	S7
Figure S11	<i><sup>1</sup>H NMR spectrum (300 MHz, CDCl<sub>3</sub>+C<sub>5</sub>D<sub>5</sub>N) of LG25.</i>	S8
Figure S12	<i>MALDI-TOF of LG25.</i>	S8
Figure S13	<i><sup>1</sup>H NMR spectrum (300 MHz, CDCl<sub>3</sub>+C<sub>5</sub>D<sub>5</sub>N) of LG26.</i>	S9
Figure S14	<i>MALDI-TOF of LG26.</i>	S9
Figure S15	<i><sup>1</sup>H NMR spectrum (300 MHz, CDCl<sub>3</sub>+C<sub>5</sub>D<sub>5</sub>N) of LG27.</i>	S10
Figure S16	<i>MALDI-TOF of LG27.</i>	S10
Figure S17	<i>Theoretical absorption spectra of LG24-LG27 Dyes by using B3LYP method PCM model in tetrahydrofuran solvent with B3LYP/6-31G(d,p) method.</i>	S11
Figure S18	<i>Singlet excited-state lifetimes of LG24, LG25, LG26 and LG27 in THF solution</i>	S12
Figure S19	<i>Reduction spectra of LG24, LG25, LG26 and LG27.</i>	S12
Figure S20	<i>Oxidative OTTLE studies porphyrin sensitizers in 0.3M TBAP/THF with an</i>	S13

	<i>applied potential of +0.90V (vs. SCE/KCl)</i>	
Figure S19.	Isodensity (0.02) plots of FMOs and the energy values in eV by using the B3LYP method 6-31G(d,p).	S14
Figure S22	<i>Photocurrent action spectra porphyrin sensitizers using different concentrations of 4-tert butylpyridine.</i>	S15
Figure S23	<i>Current–voltage characteristics of porphyrin sensitizers using different concentrations of 4-tert butylpyridine.</i>	S15
Figure S24	<i>TG/DTG curves of <b>LG24</b>, <b>LG25</b>, <b>LG26</b> and <b>LG27</b> porphyrins with heating rate 10 °C.min<sup>-1</sup> under nitrogen</i>	S16
Table S1	Optimized energies, HOMO-LUMO energies and ground state dipole moment by DFT studies by using B3LYP/6-31G (d,p) in vacuum.	S16
Table S2	Singlet excited state properties of dyes by B3LYP method function in tetrahydrofuran solvent in PCM model. <sup>a</sup> Total minimum energy of dyads and triad, <sup>b</sup> values in eV, <sup>c</sup> values in debye units.	S17

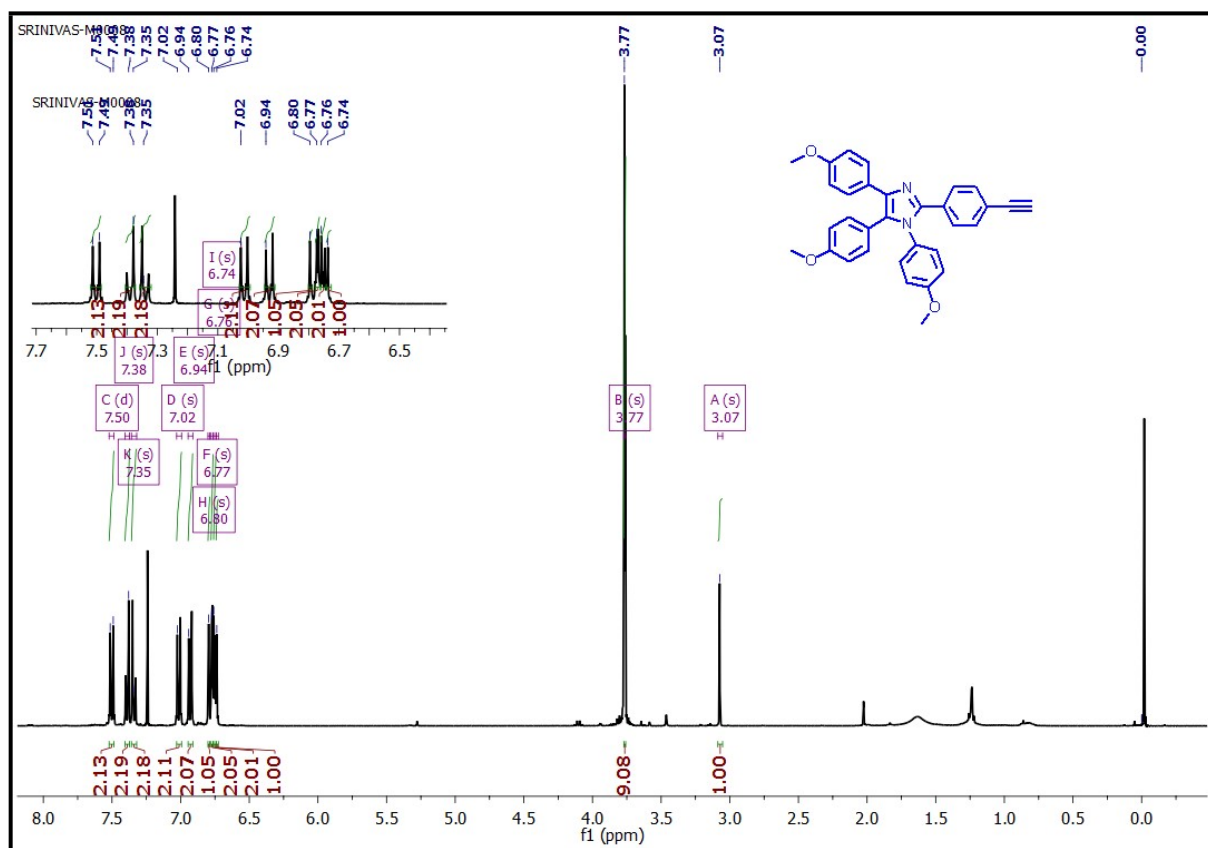


Figure S1.  $^1\text{H}$  NMR spectrum (500 MHz,  $\text{CDCl}_3$ ) of **D1**.

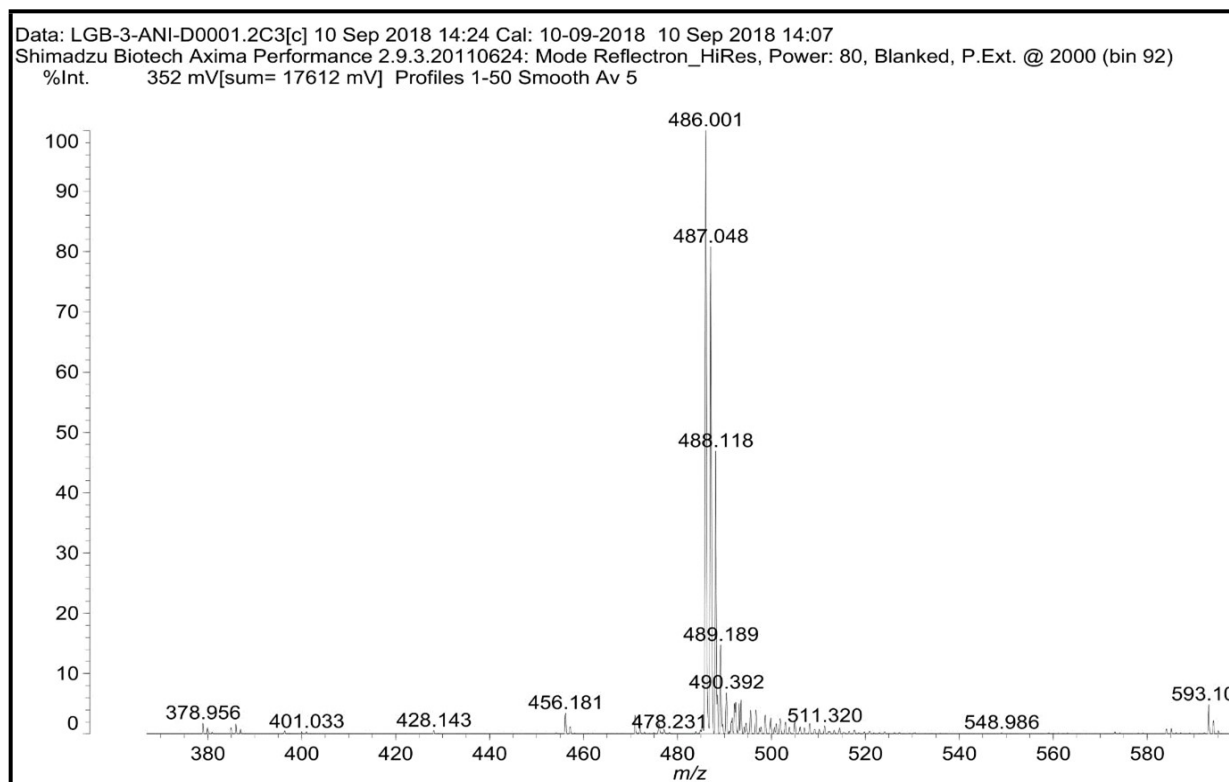


Figure S2. ESI-MS of **D1**

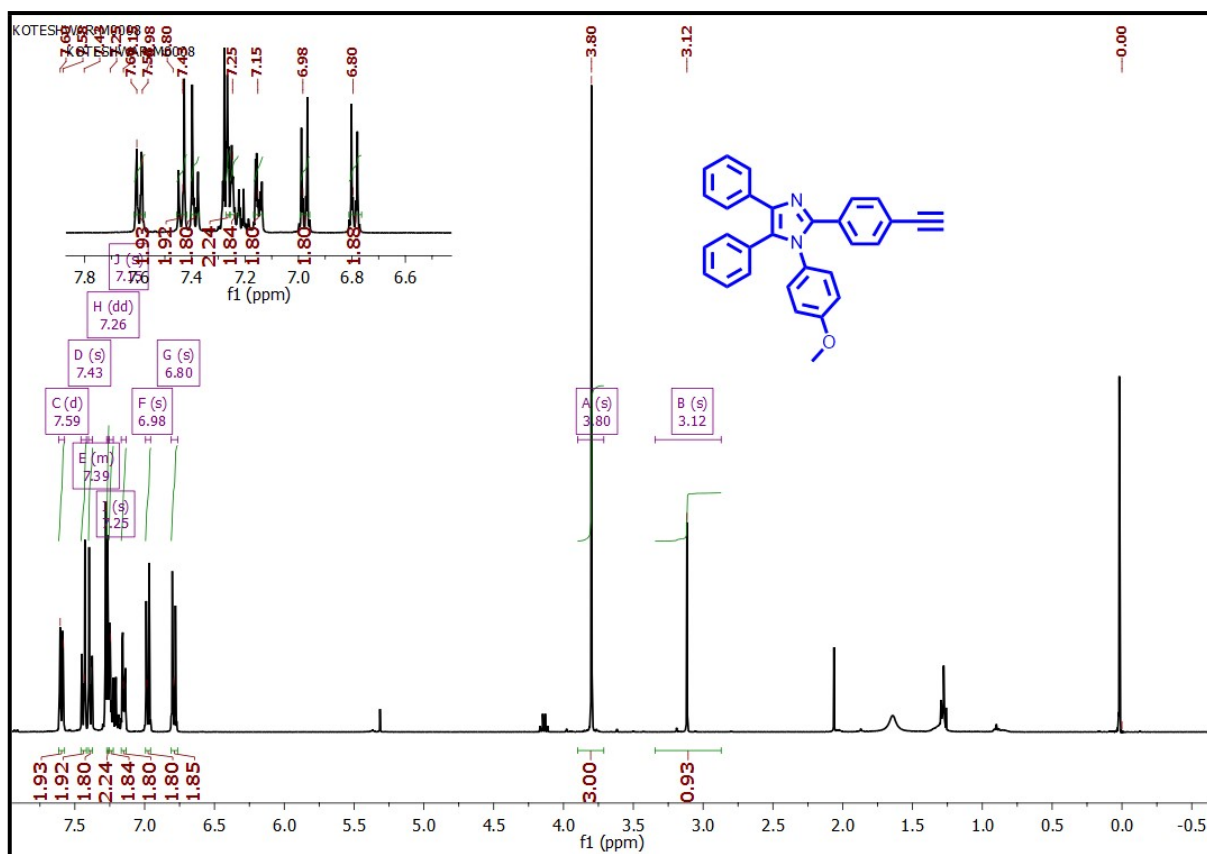


Figure S3.  $^1\text{H}$  NMR spectrum (500 MHz,  $\text{CDCl}_3$ ) of **D2**.

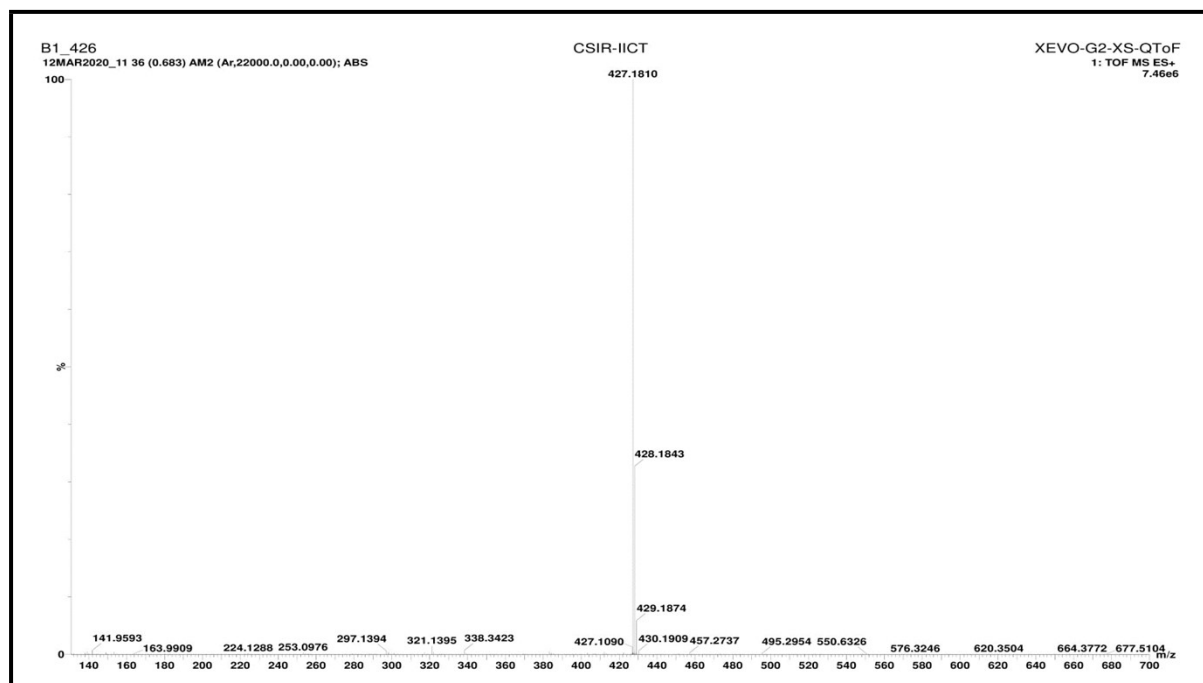


Figure S4. ESI-MS of **D2**.

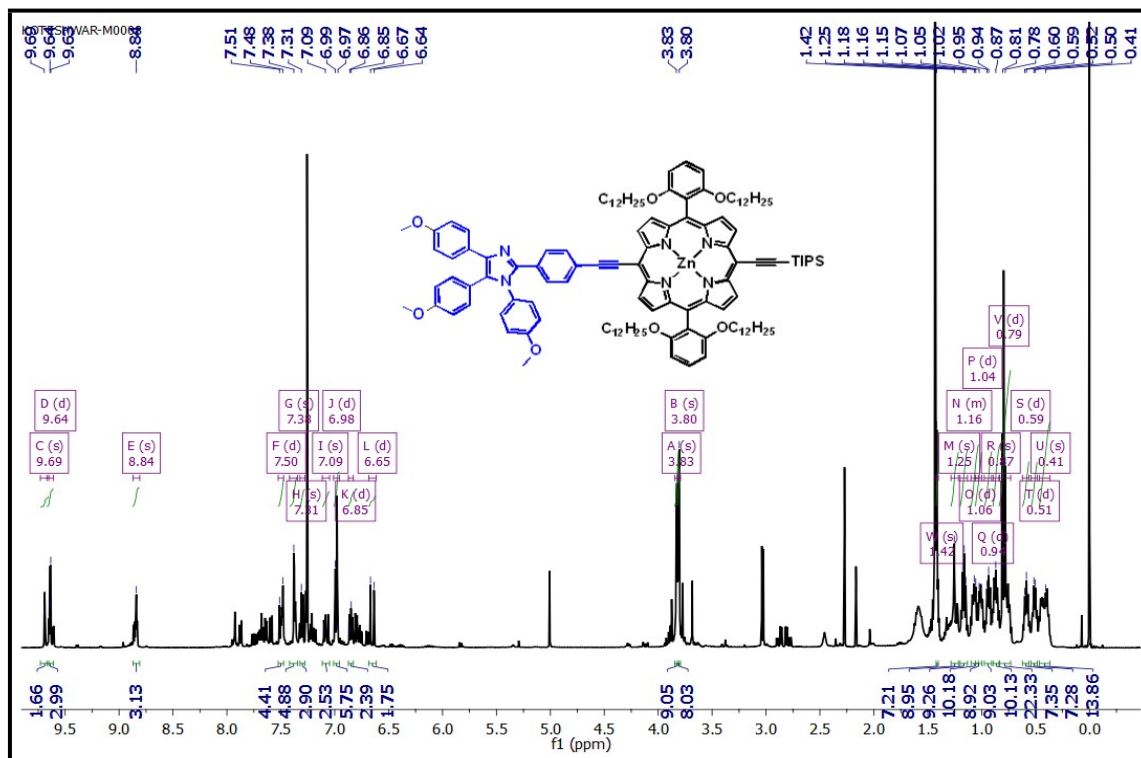


Figure S5. <sup>1</sup>H NMR spectrum (500 MHz, CDCl<sub>3</sub>) of 3.

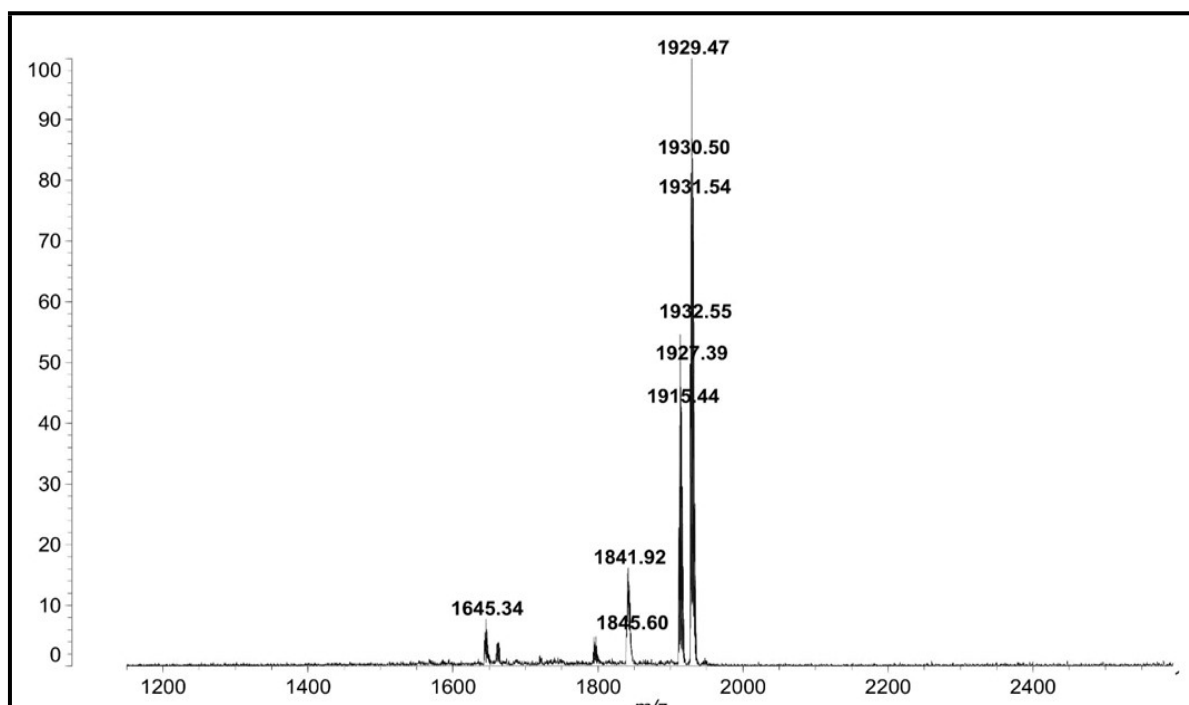


Figure S6. MALDI-TOF of 3.

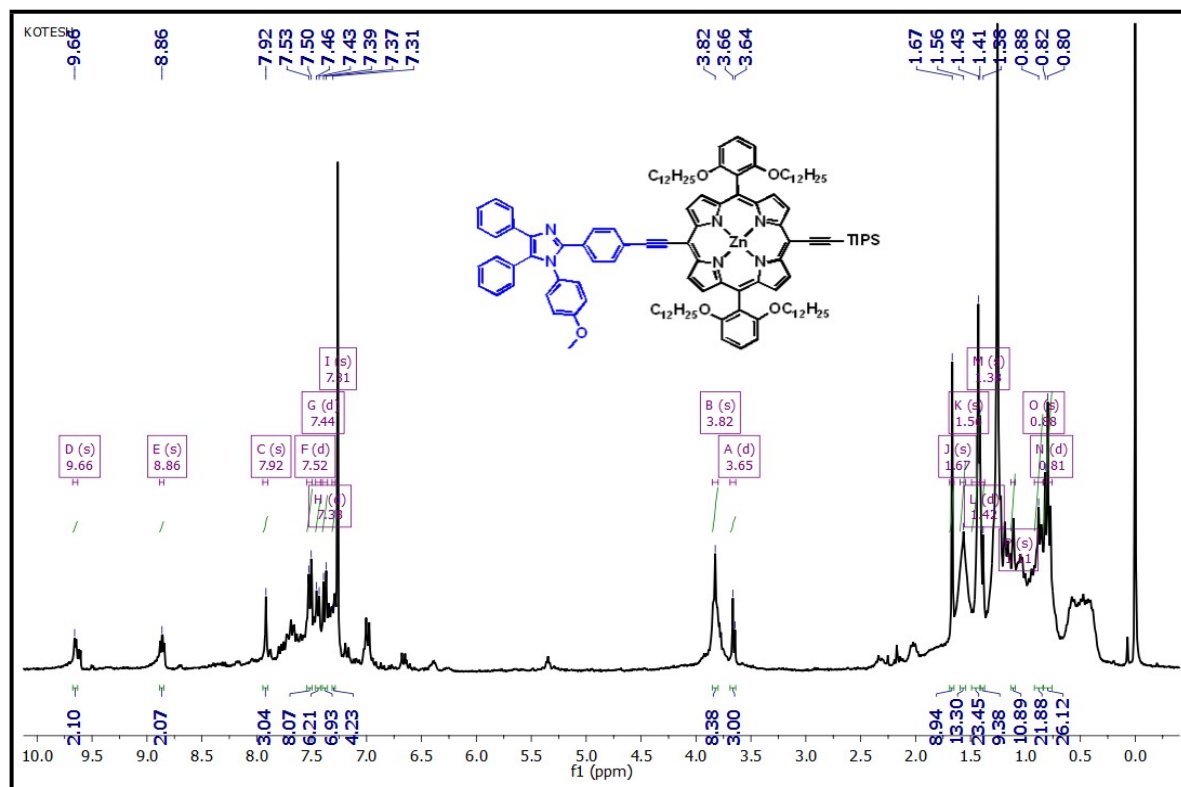


Figure S7.  $^1H$  NMR spectrum (500 MHz,  $CDCl_3$ ) of 4.

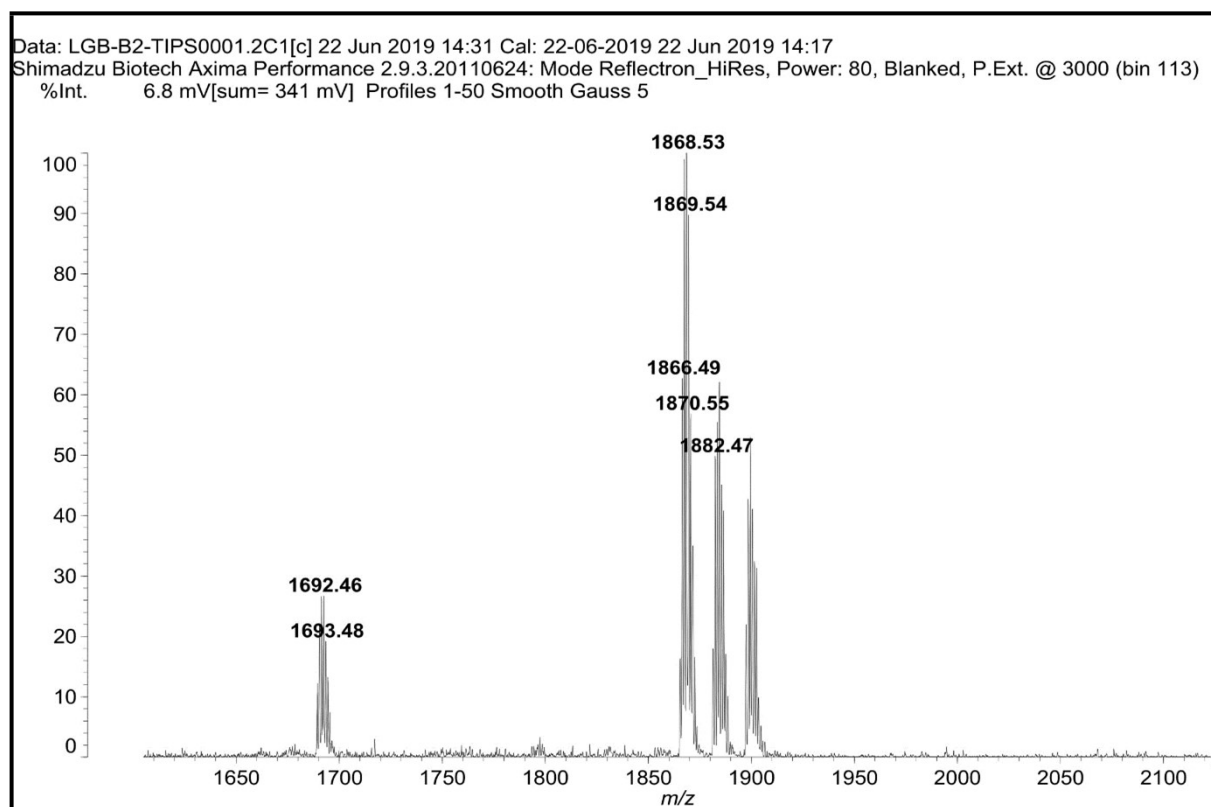


Figure S8. MALDI-TOF of 4.

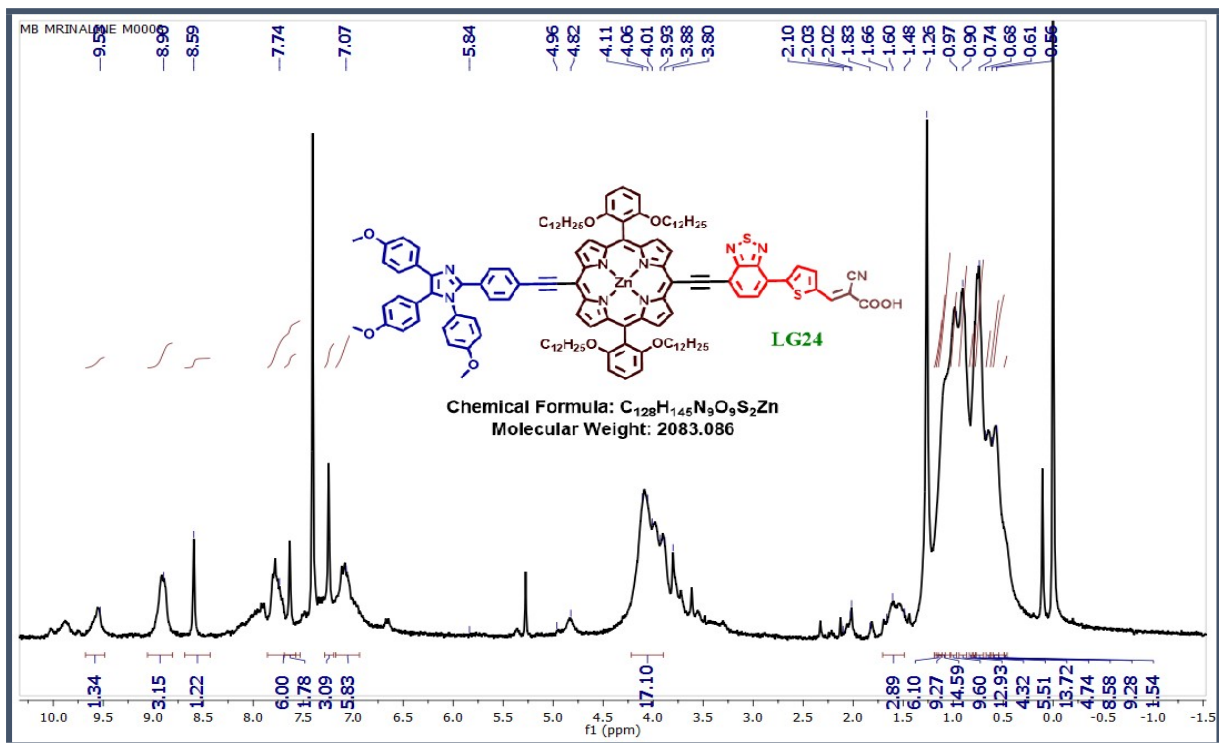


Figure S9.  $^1H$  NMR spectrum (500 MHz,  $CDCl_3$ ) LG24

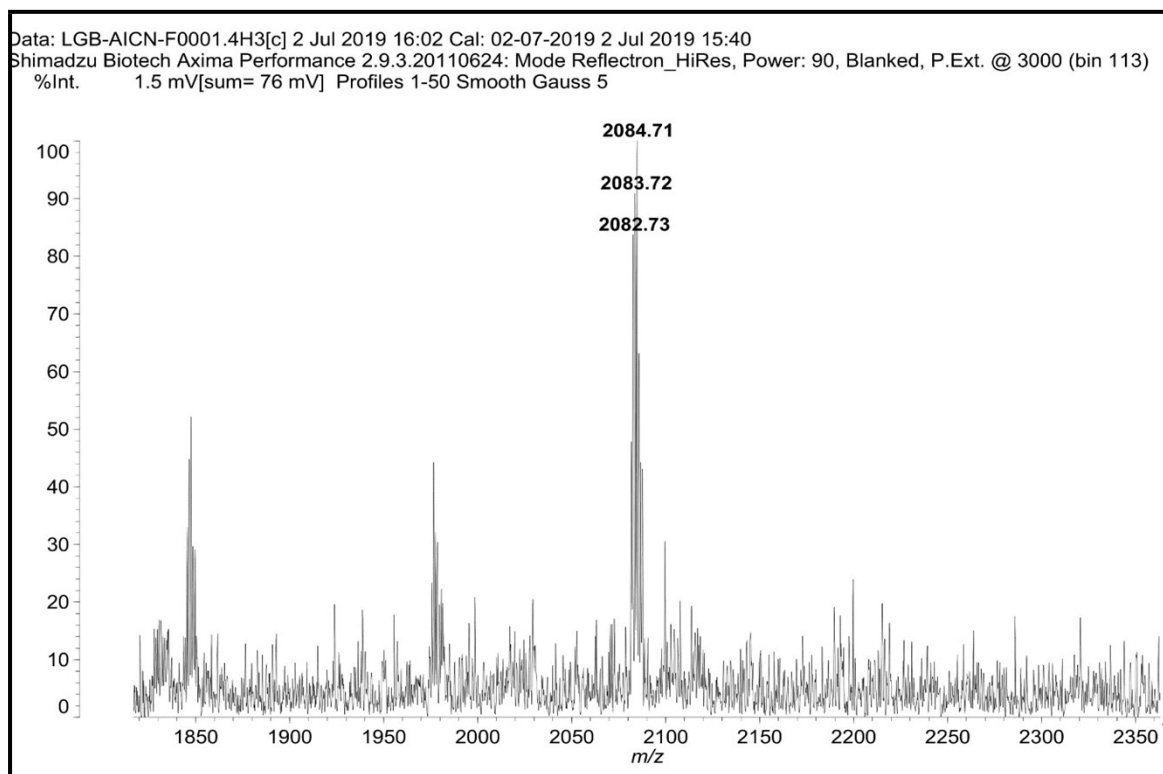


Figure S10. MALDI-TOF of LG24.

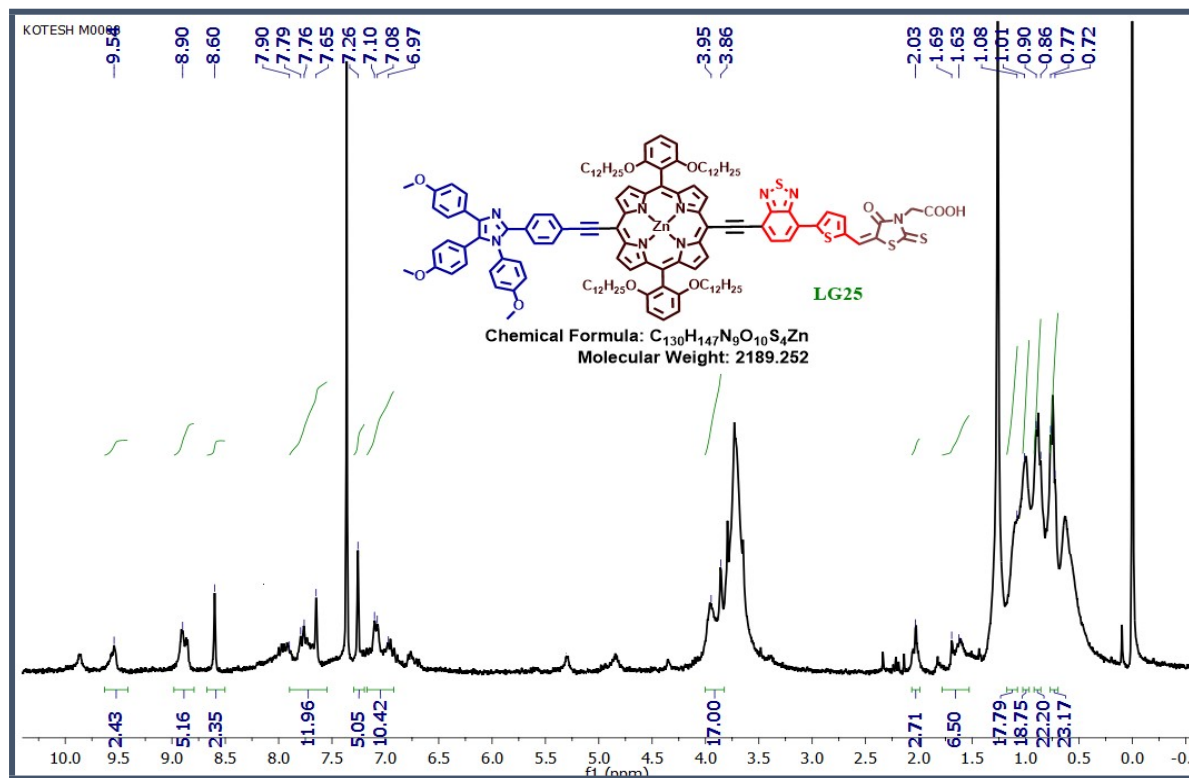


Figure S11.  $^1H$  NMR spectrum (500 MHz,  $CDCl_3$ ) of LG25.

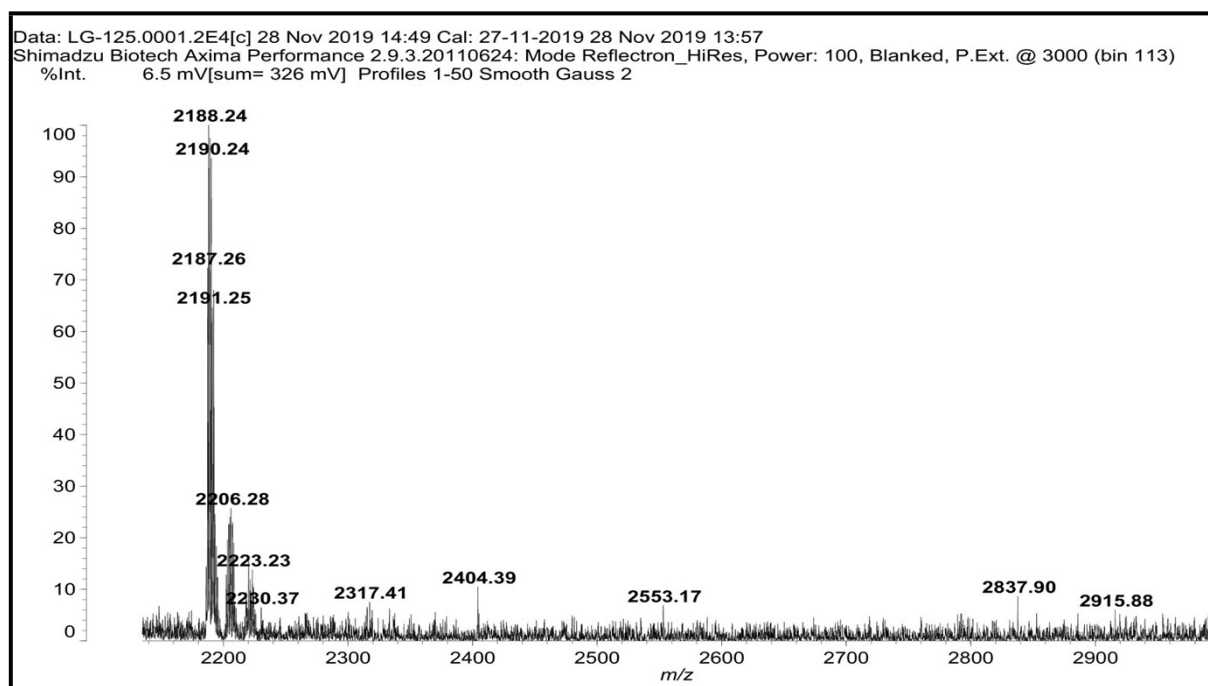


Figure S12. MALDI-TOF of LG25.

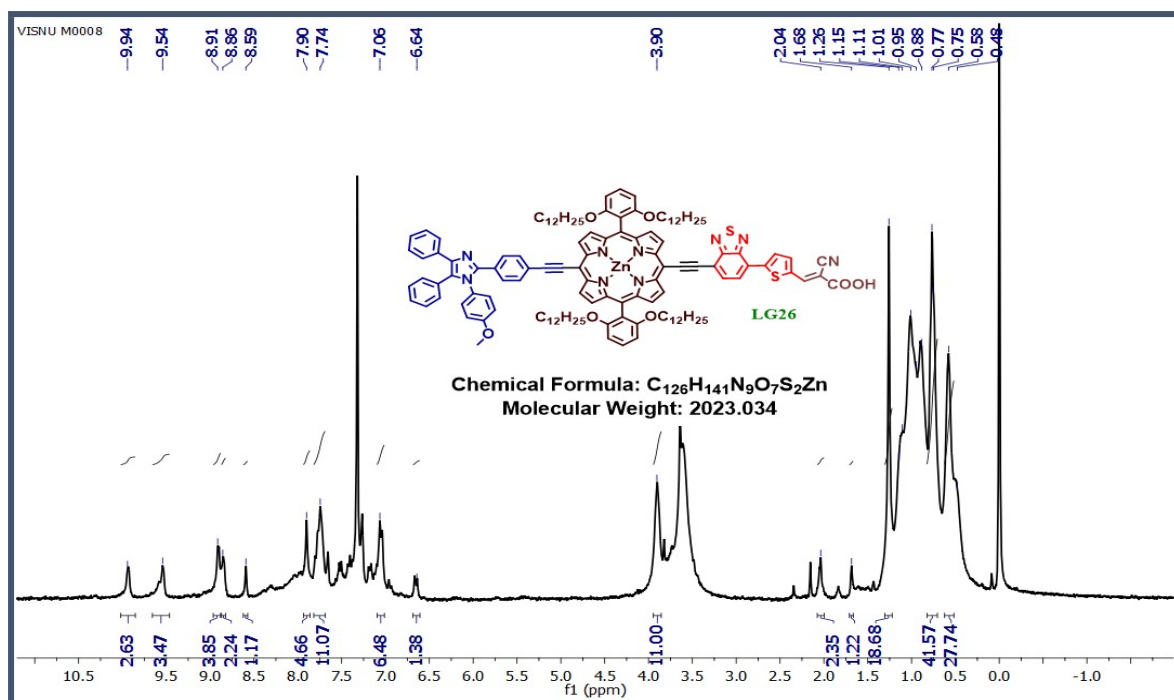


Figure S13.  $^1H$  NMR spectrum (500 MHz,  $CDCl_3$ ) of LG26.

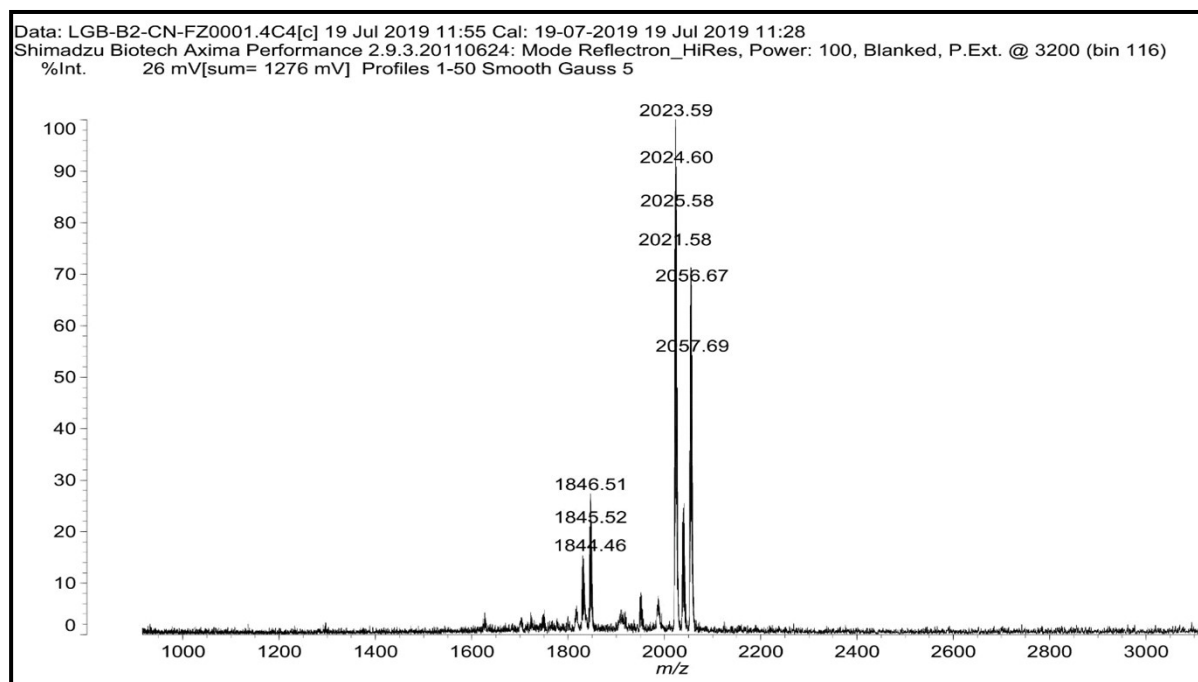


Figure S14. MALDI-TOF of LG26.

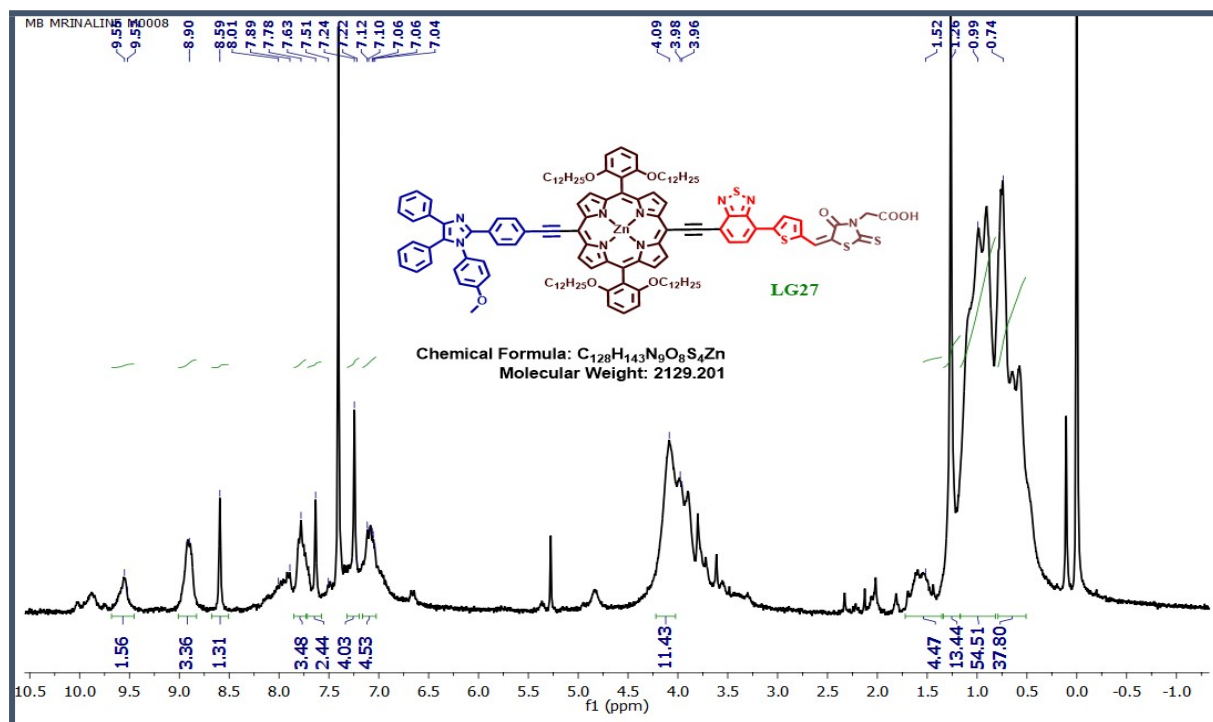


Figure S15.  $^1H$  NMR spectrum (500 MHz,  $CDCl_3$ ) of LG27.

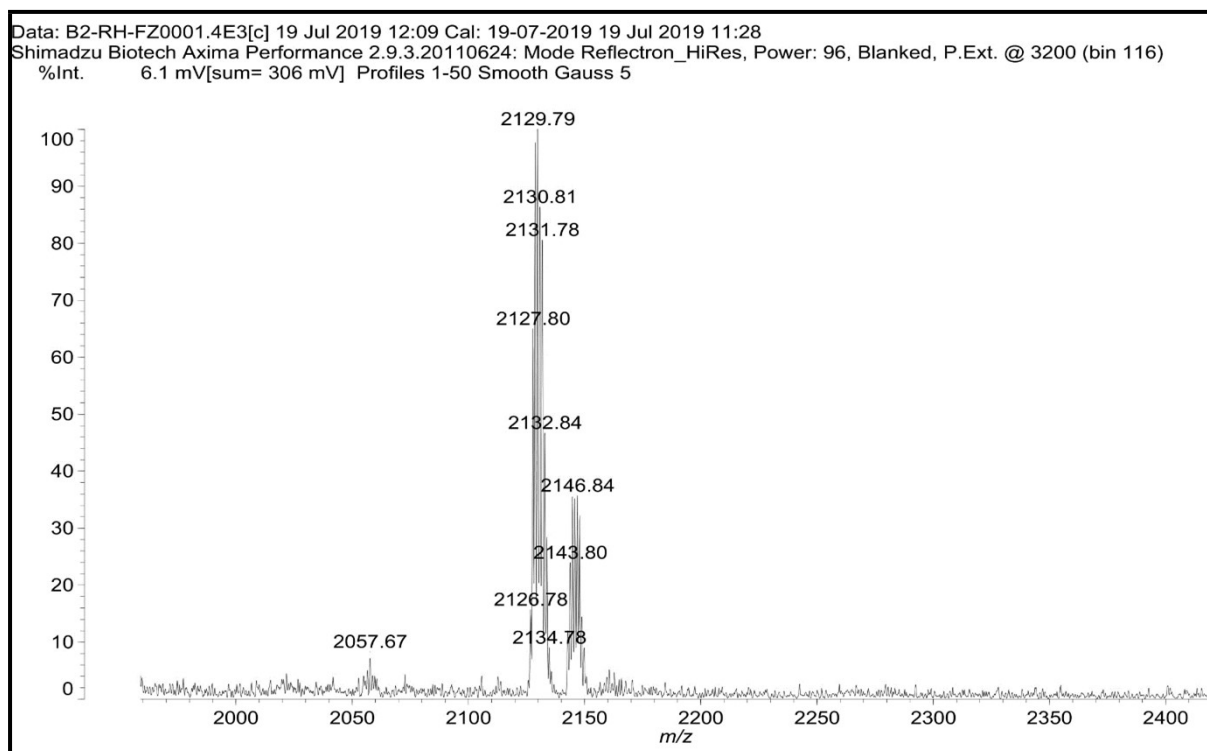
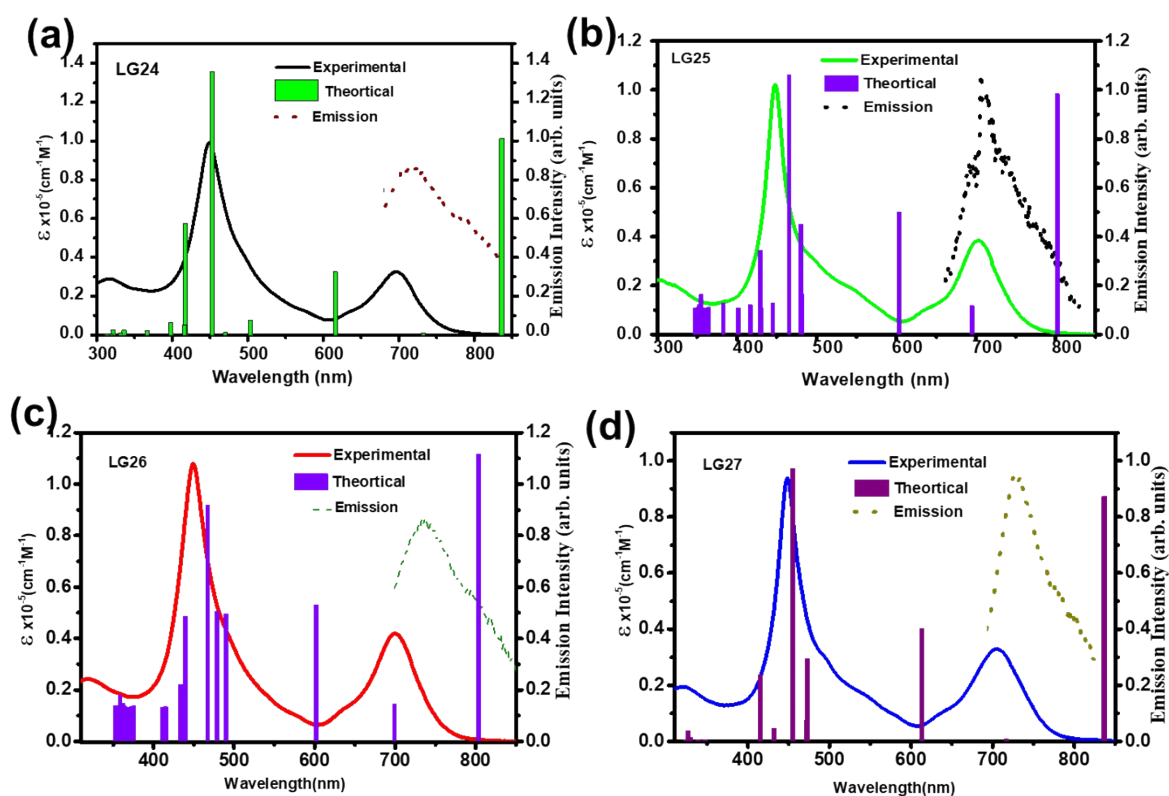


Figure S16. MALDI-TOF of LG27.



**Figure S17.** Theoretical absorption spectra of **LG24-LG27** Dyes by using B3LYP method PCM model in tetrahydrofuran solvent with B3LYP/6-31G(d,p) method.

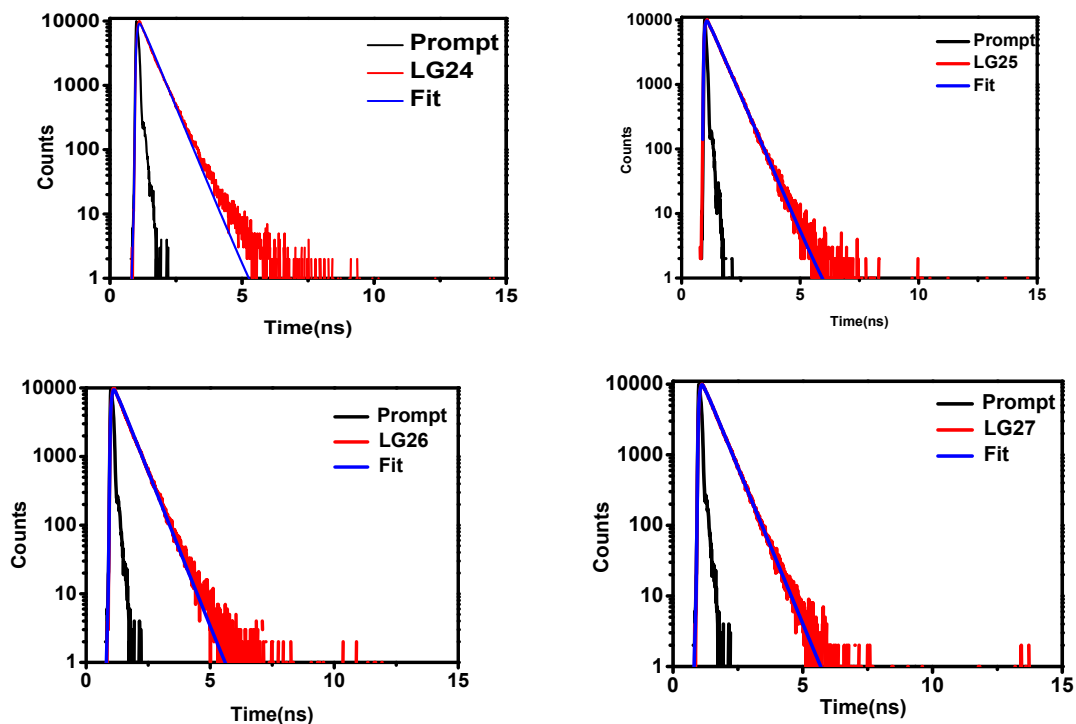


Figure S18. Singlet excited-state lifetimes of LG24, LG25, LG26 and LG27 in THF solution

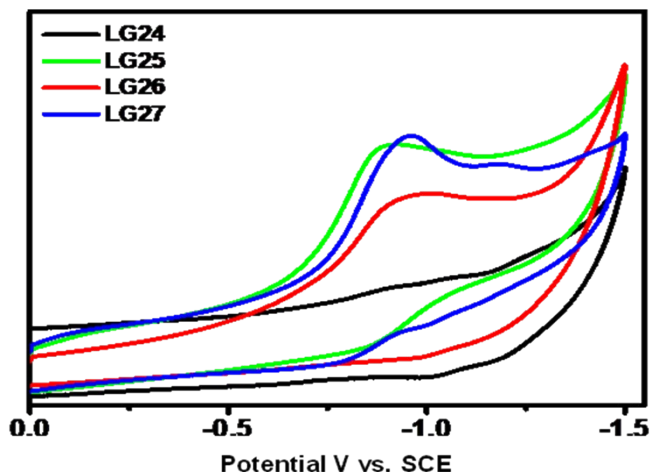
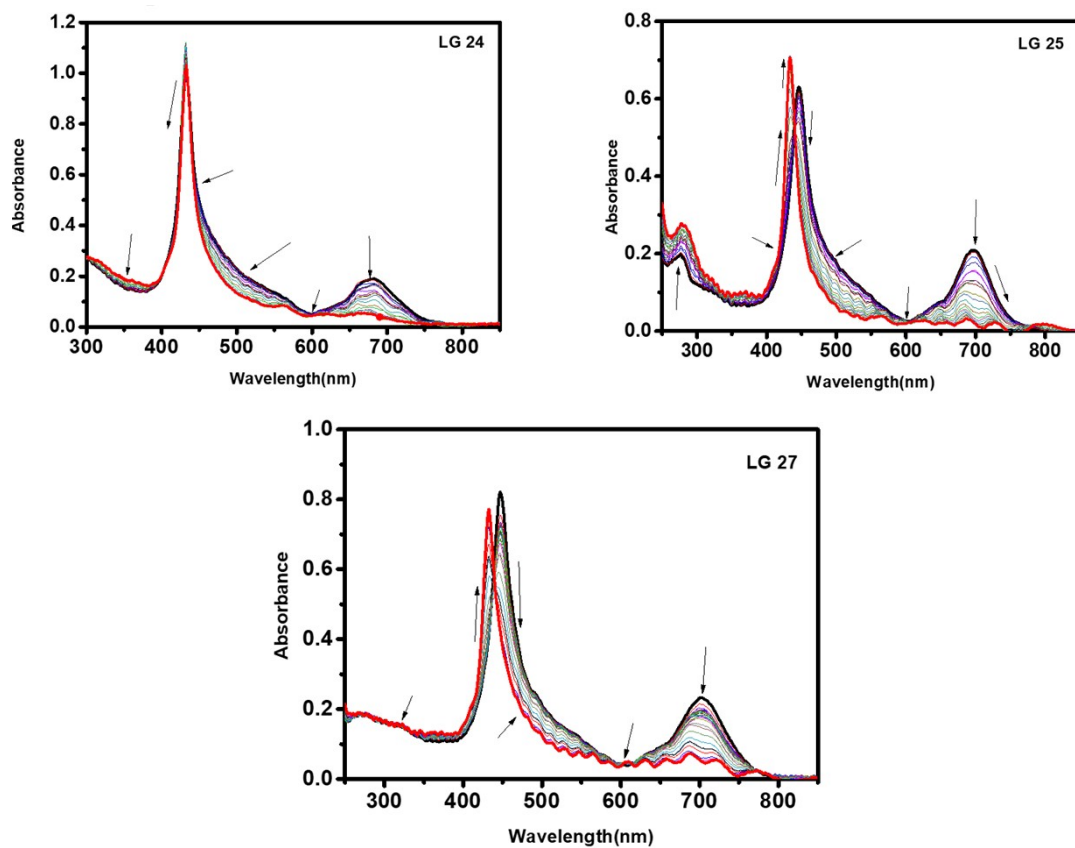
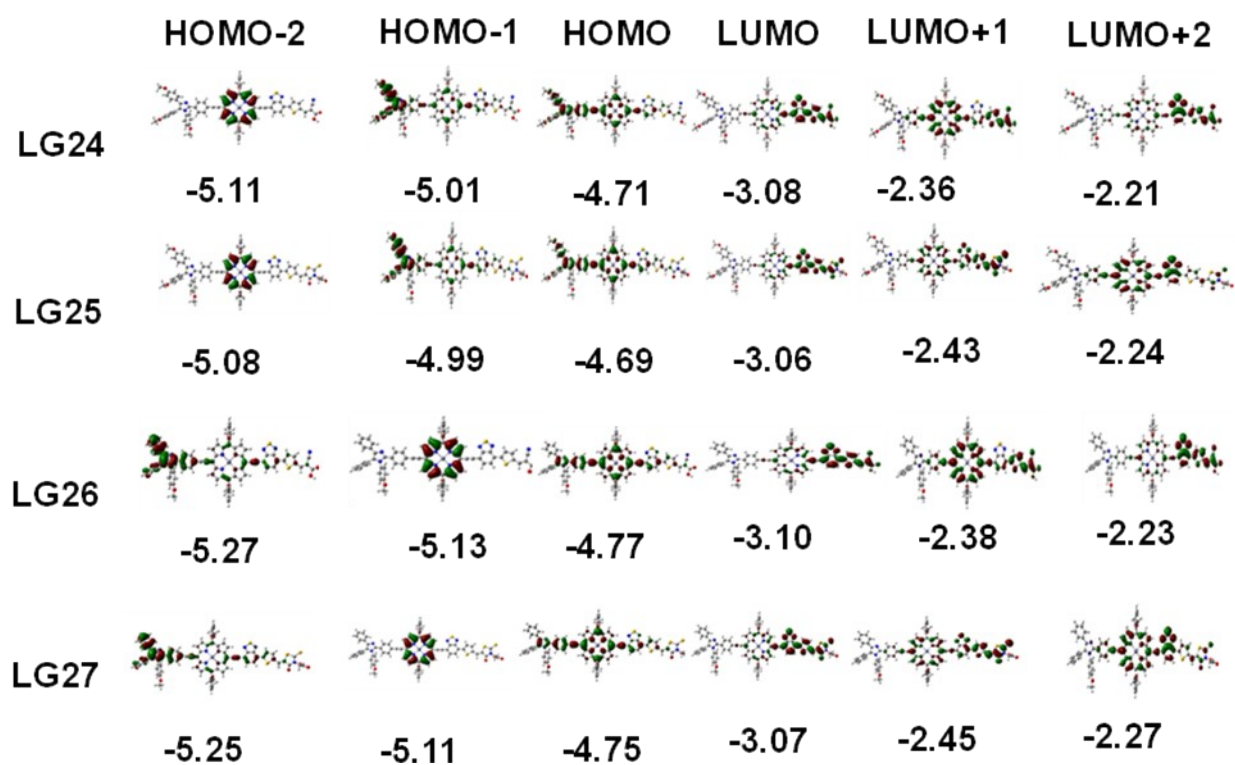


Figure S19. Reduction spectra of LG24, LG25, LG26 and LG27 in THF.



**Figure S20.** Oxidative OTTLE studies of **LG24**, **LG25**, **LG27** series sensitizers in 0.3M TBAP/THF with an applied potential of +0.95V (vs. SCE/KCl).



**Figure S21.** Isodensity (0.02) plots of FMOs and the energy values in eV by using the B3LYP method 6-31G(d,p).

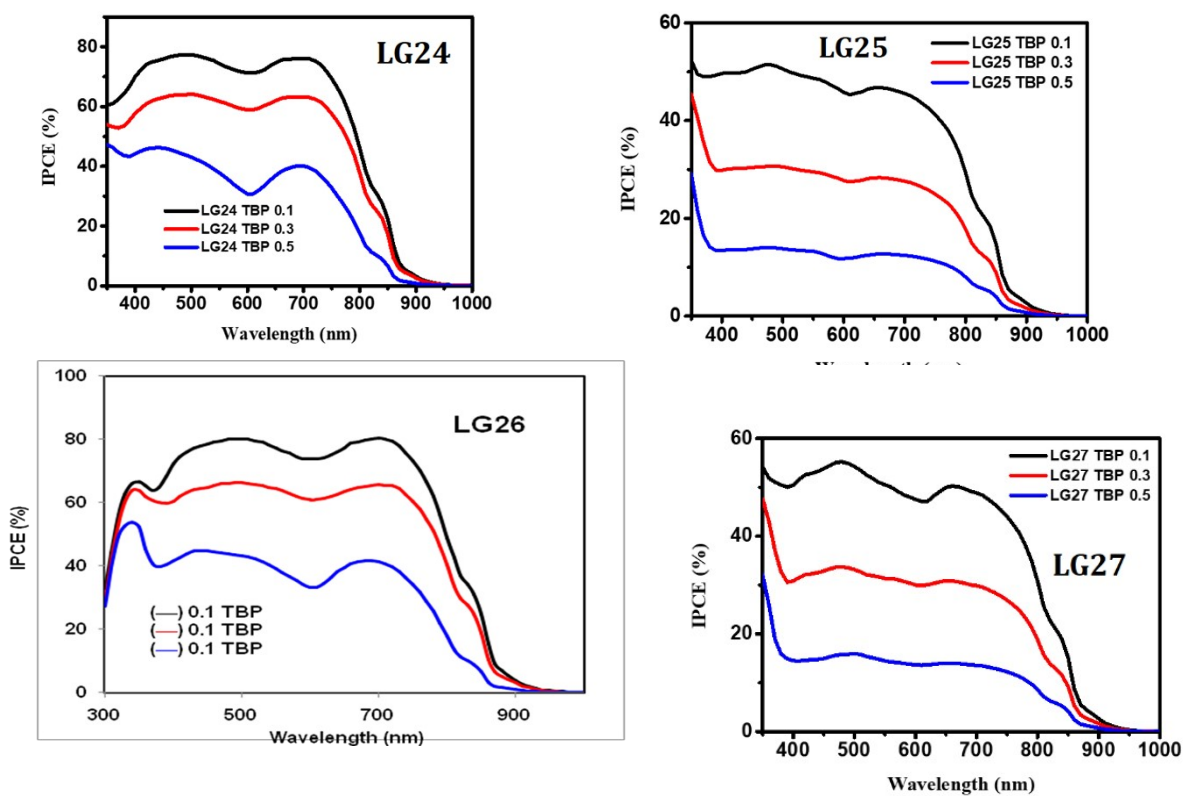


**Figure S22.** Photocurrent action spectra porphyrin sensitizers using different concentrations of 4-tert butylpyridine.

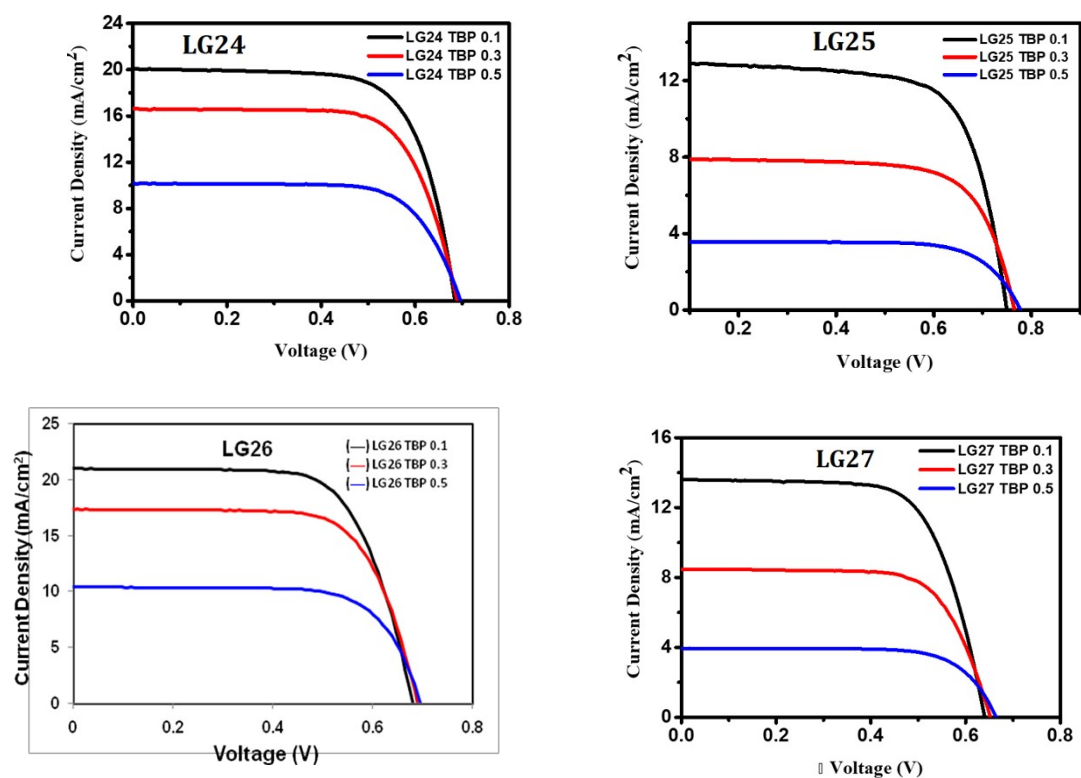


**Figure S23.** Current–voltage characteristics of porphyrin sensitizers using different concentrations of 4-*tert* butylpyridine.

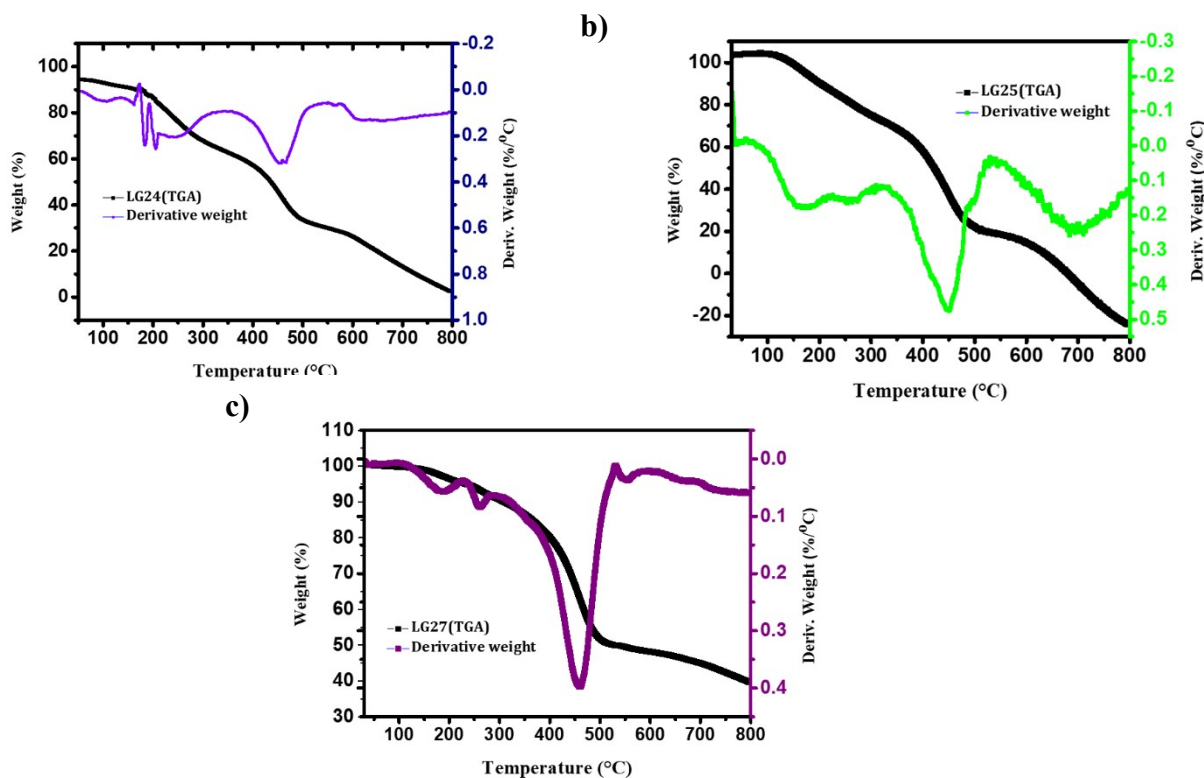


**Figure S24.** TG/DTG curves of **LG24**, **LG25** and **LG27** porphyrins with heating rate  $10\text{ }^{\circ}\text{C}\cdot\text{min}^{-1}$  under nitrogen.

**Table 1:** Optimized energies, HOMO-LUMO energies and ground state dipole moment by DFT studies by using B3LYP/6-31G (d,p) in vacuum.

Dye	<sup>a</sup> <i>E</i> , K.cal./mol	<sup>b</sup> HOMO (H),	<sup>b</sup> LUMO (L)	<sup>b</sup> H-Lgap	<sup>c</sup> μ
<b>LG24</b>	-4380303	-4.74	-3.08	1.66	17.517
<b>LG25</b>	-4975847	-4.69	-3.06	1.63	16.047
<b>LG26</b>	-4236628	-4.77	-3.10	1.67	15.372
<b>LG27</b>	-4832119	-4.75	-3.07	1.68	13.477

<sup>a</sup>Total minimum energy of **LG24-LG27**, <sup>b</sup>values in eV, <sup>c</sup>values in debye units.

**Table 2:** Singlet excited state properties of dyes by B3LYP method in tetrahydrofuran solvent in PCM model.

Dye	<sup>a</sup> $\lambda_{\max}$	<sup>b</sup> $f$	<sup>c</sup> E (eV)	% of Molecular Orbital Contribution
<b>LG24</b>	430	0.128	2.878	H-1->LUMO (59%), H-1->L+1 (11%), HOMO->L+3 (17%) H-1->L+2 (4%), HOMO->L+2 (5%)
	583	0.016	2.123	H-1->LUMO (38%), H-1->L+1 (27%), HOMO->L+3 (24%) HOMO->L+2 (7%)
	653	1.689	1.898	HOMO->LUMO (64%), HOMO->L+1 (16%) H-3->LUMO (3%), H-2->LUMO (3%), H-1->L+3 (8%)
<b>LG25</b>	415	0.131	2.986	H-3->LUMO (33%), H-1->L+2 (23%), HOMO->LUMO (13%)H-7->L+1 (4%), H-3->L+1 (3%), H-2->LUMO (9%), HOMO->L+3 (4%)
	580	0.018	2.136	H-1->LUMO (36%), H-1->L+1 (25%), HOMO->L+2 (34%)
	662	2.00	1.870	HOMO->LUMO (66%), HOMO->L+1 (15%)H-3->L+1 (3%), H-2->LUMO (3%), H-1->L+2 (9%)
<b>LG26</b>	416	0.679	2.977	H-1->LUMO (51%), HOMO->L+2 (46%)
	581	0.021	2.132	H-1->LUMO (38%), H-1->L+1 (25%), HOMO->L+2 (33%)
	663	1.845	1.869	HOMO->LUMO (69%), HOMO->L+1 (14%) H-3->L+1 (3%), H-2->LUMO (2%), H-1->L+2 (9%)
<b>LG27</b>	413	0.672	2.995	H-1->LUMO (44%), HOMO->L+2 (43%) H-3->LUMO (3%), H-1->L+2 (2%)
	580	0.041	2.196	H-1->LUMO (37%), H-1->L+1 (24%), HOMO->L+2 (34%)

<sup>a</sup>Theoretical absorbance in nm, <sup>b</sup>Oscillator strength, and <sup>c</sup>Excited state energy in eV.